Pis'ma v ZhETF, vol. 102, iss. 4, pp. 281 – 286

Optical storage based on coupling of one-way edge modes and cavity modes

Y. Fang[+], *Zh. Ni*[+], *H. Q. He*[+], *T. Jiang*[*1)]

[+]*School of Computer Science and Telecommunication Engineering, Jiangsu University, 212013 Zhenjiang, China*

[*]*School of Statistics and Mathematics, Zhejiang Gongshang University, 310018 Hangzhou, China*

Submitted 5 June 2015
Resubmitted 7 July 2015

We design a new kind of optical storage composed of a ring resonator that is based on both the one-way property of the edge modes of magneto-optical photonic crystals and the coupling effect of cavities. The ring resonator can be served as an optical storage through a close field circulation. Through another edge waveguide and coupling cavity, the electromagnetic signals can be either written into the storage or be taken out from it.

DOI: 10.7868/S0370274X15160122

I. Introduction. For many years scientists believed that "optical data cannot be stored statically and must be processed and switched on the fly". The reason for this conclusion was that the speed of light is so fast that stopping and storing an optical signal is thought to be impossible. However, recent progresses of science and technology annulled such assertions and prove that the group velocity of light can be decelerated to zero, effectively trapping or "stopping" the light pulse [1]. In addition, the ring resonator has been widely used in the development of microwave bandpass filters, couplers, mixers, oscillators, and antennas. The ring resonators combined with other waveguides make light circulating along a single direction, which has useful roles in modulating optical circuits [2–4]. However, the early ring resonator systems have many ports and the optical flow cannot be formed in a close path. Thus, the conventional ring resonator can not be used as a storage system. If the optical flow is circulated in an isolated ring resonator in a close path, the optical data can be saved. Thus, besides "trapping" or "stopping" the light pulse, another way for dynamically storing optical data may be with the help of the new ring resonator. To design such new ring resonator is the subject of this study. In addition, basing on the new ring resonator we will design an optical storage.

Our idea comes from the existence of one-way electromagnetic modes in 2D magneto-optical (MO) photonic crystals similar to the chiral edge states found in the integer quantum Hall (QH) effect [5, 6]. Also, Zheng Wang et al. demonstrated the unidirectional edge modes through experimental and theoretical study [7–9]. These modes are confined at the edge of certain 2D MO photonic crystals and possess group velocities pointing in only one direction, determined by the direction of an applied dc magnetic field. Backscattering in the unidirectional edge modes is completely suppressed. As is well known, the coupling among different modes may excite many new and interesting phenomena. In this study we try to make the coupling of the unidirectional edge modes and cavity modes in order to achieve a new kind of ring resonator and find some new transmission mechanism.

II. Structure and method. We use a truncated 2D MO PC with its two edges combined with two regular PCs. All the dielectric rods extend along the z direction and the cross plane is the xy plane. The structure may excite two unidirectional edge modes on the two edges of the 2D MO PCs, respectively. Two regular PCs are used as gapped layers to prevent light scattering into air. The two edge modes may be independent if the interval of the two edges is large enough. The structure parameters for the 2D MO PC are the same as those in Ref. [7]. A square lattice of YIG rods ($\varepsilon = 15\varepsilon_0$) of radius $0.11a$ in air is considered, where a is the lattice constant. The regular PCs consist of a square lattice of alumina rods with dielectric constant $\varepsilon = 10\varepsilon_0$ in air background, and its lattice direction is with 45° to the YIG lattice. The regular PC lattice constant is $a/\sqrt{2}$ and the alumina rod radius is $0.106a$. An external direct current (dc) magnetic field applied in the out-of-plane (z) direction induces strong gyromagnetic anisotropy, with the permeability tensor taking the form [7]

1) e-mail: jtao@263.net

$$\mu(\mathbf{r}) = \begin{bmatrix} \mu_1 & j\mu_2 & 0 \\ -j\mu_2 & \mu_1 & 0 \\ 0 & 0 & \mu_3 \end{bmatrix}, \tag{1}$$

where $\mu_1 = 14\mu_0$, $\mu_2 = 12.4\mu_0$. The two edge modes of the 2D MO PC can be obtained from the modified plane wave expansion method. For $\mathbf{E}$ polarization (the electric field is along the z axis), we eliminate the magnetic field from Maxwell's equations to obtain the wave equation

$$\nabla \times \frac{1}{\mu(\mathbf{r})} \nabla \times \mathbf{E}(\mathbf{r}) = \omega^2 \varepsilon(\mathbf{r}) \varepsilon_0 \mu_0 \mathbf{E}(\mathbf{r}) = \varepsilon(\mathbf{r}) \frac{\omega^2}{c^2} \mathbf{E}(\mathbf{r}), \tag{2}$$

where $\frac{1}{\mu(\mathbf{r})} = \begin{bmatrix} \mu' & j\mu'' & 0 \\ -j\mu'' & \mu' & 0 \\ 0 & 0 & \mu''' \end{bmatrix}$ and $\varepsilon_{(\mathbf{r})}$ are the position-dependent periodic structure in the xy plane. Taking advantage of the periodic nature of the problem, the E-field may be expanded into a sum of plane waves using Bloch's theorem as

$$E_z(\mathbf{r}) = \sum_{\mathbf{G}} E(\mathbf{k}+\mathbf{G}) \exp[i(\mathbf{k}+\mathbf{G}) \cdot \mathbf{r}], \tag{3}$$

where $\mathbf{k}$ is a wave vector in the Brillouin zone, $\mathbf{G}$ represents a lattice vector in reciprocal space (also a square lattice), describing the periodic structure, and $\mathbf{E}(\mathbf{k}+\mathbf{G})$ is the expansion coefficient corresponding to $\mathbf{G}$. The tensor elements of $1/\mu(\mathbf{r})$ can be expressed as a Fourier series expansion [10, 11]

$$\mu' = \sum_{\mathbf{G}} \mu'(\mathbf{G}) \exp(i\mathbf{G} \cdot \mathbf{r}), \tag{4}$$

$$\mu'' = \sum_{\mathbf{G}} \mu''(\mathbf{G}) \exp(i\mathbf{G} \cdot \mathbf{r}), \tag{5}$$

where

$$\mu'(\mathbf{G}) = \frac{1}{A_u} \int \mu'(\mathbf{r}) \exp(-i\mathbf{G} \cdot \mathbf{r}) d\mathbf{r}, \tag{6}$$

$$\mu''(\mathbf{G}) = \frac{1}{A_u} \int \mu''(\mathbf{r}) \exp(-i\mathbf{G} \cdot \mathbf{r}) d\mathbf{r}. \tag{7}$$

In (6), (7) A_u indicates the area of Wigner–Seitz (WS) unit cell that may be used to represent the periodic structure. By taking Eqs. (3)–(5) into (2), we finally obtain

$$\sum_{\mathbf{G}'} [\mu'(\mathbf{G}-\mathbf{G}')\mathbf{K}' \cdot \mathbf{K} - j\mu''(\mathbf{G}-\mathbf{G}')(\mathbf{K}' \times \mathbf{K} \cdot \mathbf{e}_z)] E(\mathbf{k}+\mathbf{G}') =$$

$$= \frac{\omega^2}{c^2} \sum_{\mathbf{G}'} \varepsilon(\mathbf{G}-\mathbf{G}') E(\mathbf{k}+\mathbf{G}'), \tag{8}$$

where $\mathbf{K} = \mathbf{k}+\mathbf{G}$, $\mathbf{K}' = \mathbf{k}+\mathbf{G}'$, and

$$\varepsilon(\mathbf{G}-\mathbf{G}') = \frac{1}{A_u} \int \varepsilon(\mathbf{r}) \exp[-i(\mathbf{G}-\mathbf{G}') \cdot \mathbf{r}] d\mathbf{r}, \tag{9}$$

Eq. (8) includes the sum of infinite number of reciprocal vectors $\mathbf{G}'$ and we select finite reciprocal vectors instead in the allowed precision range. Then the equation becomes a matrix eigenvalue equation. For a fixed wave vector $\mathbf{k}$, the frequencies ω of the allowed modes in the periodic structure are found through solving Eq. (8). In the band calculations for the edge modes, a supercell must be used. Theoretically, the supercell must contain infinite rods. In practical calculations a finite number of rods can satisfy the needed accuracy.

III. Results and analysis. According to Eqs. (1)–(8), we calculate the projected band diagram of the structure system. The 2D MO PC has a width of $6a$. The band diagram for the compound structure is shown in Fig. 1a. There are two symmetric dispersion curves in the common gap of the MO PC and the regular PC. The red dashed curve and the black solid curve correspond to the upper edge modes and the lower edge modes, respectively. Each dispersion curve has only one group velocity direction, but the two group velocity directions corresponding to the two dispersion curves are opposite. Because the two edges have enough interval and the two edge modes are not coupled, the black dispersion curve is close to the single edge modes in Ref. [7]. To give a direct illustration of the one-way edge modes, we place two point sources with frequency $\omega = 0.5417(2\pi c/a)$ at the centers of the two edges, respectively. The calculated steady-state $\mathbf{E}_z$ field distributions in Fig. 1b show that the lower source excites edge mode only propagating to the right, whereas the upper source excites edge mode only propagating to the left. The results are calculated by the finite-element frequency-domain method and the scatter boundary conditions are used.

If we set up a cavity in the MO PC, the cavity resonance may be coupled with the two edge modes, and the two edge channels can tunnel through the coupling. The cavity can be formed by increasing one rod radius denoted as r_c. The coupling only occurs when the frequency of the cavity mode is close to that of the edge mode. One of the cavity mode frequencies with $r_c = 0.33a$ is found at $\omega = 0.5522(2\pi c/a)$. Fig. 2 shows that the one-way wave from a point source with $\omega = 0.5525(2\pi c/a)$ at the lower edge channel is completely tunneled to the upper edge channel through the coupling of cavity. Because of the one-way property, the propagating directions of the two channels are opposite.

The above results provide us the design basis. It is clear that a single cavity cannot form a close circulation.

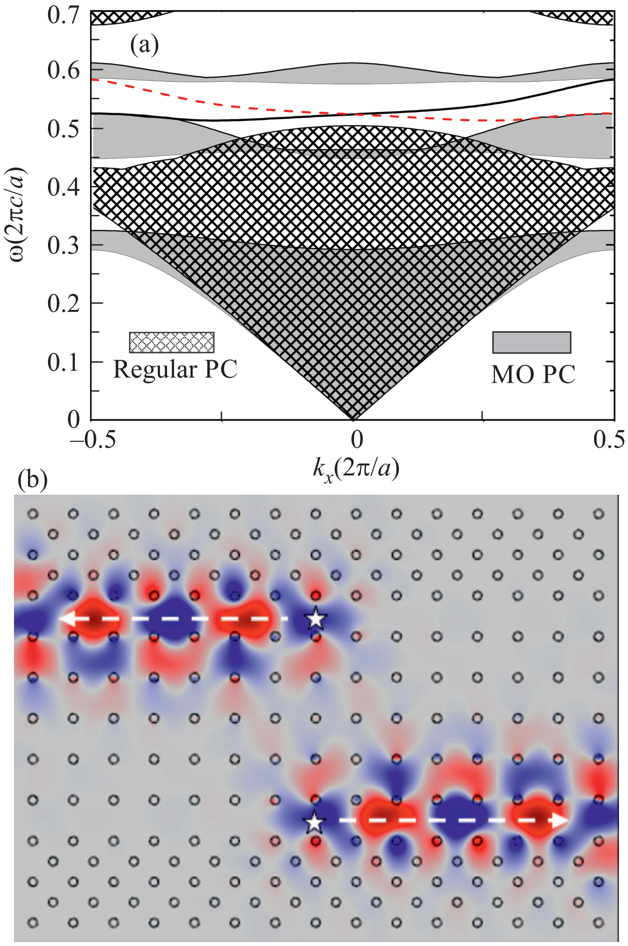

Fig. 1. (Color online) (a) – The projected band diagram of the MO PC combined with two regular PCs. The red dashed curve and the black solid curve correspond to the upper edge modes and the lower edge modes, respectively. (b) – The $\mathbf{E}_z$ field distributions from two point sources (denoted as stars) with $\omega = 0.5417(2\pi c/a)$ at the edges, respectively. The two point sources both excite one-way transmission modes with opposite directions

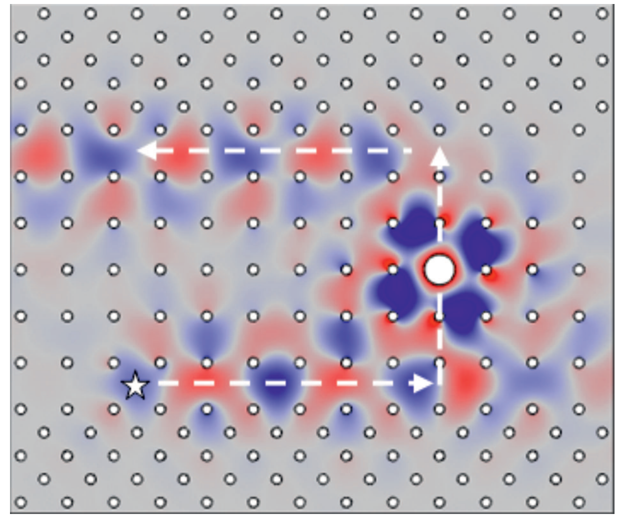

Fig. 2. (Color online) The $\mathbf{E}_z$ field distributions correspond to the tunnelling from the lower channel to the upper channel. The white arrows denote the propagation directions

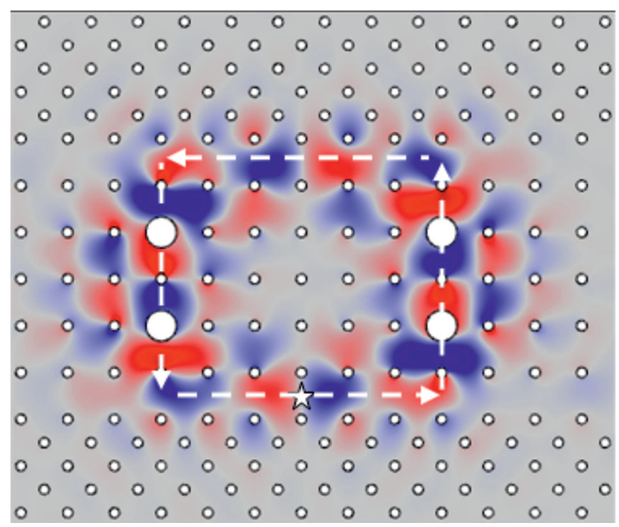

Fig. 3. (Color online) A close one-way field circulation from the coupling of two unidirectional edge modes and four cavity modes. The white arrows denote the propagation directions

To form a close ring resonator, we try to set up another cavity to the left of the existed one in Fig. 2. But we find that a close circulation has not been formed with the two cavities because the coupling intensity among the cavities and the edge channels is too small. Thus, we set up four cavities in the MO PC by changing the radius of four rods as $0.33a$. The four cavities form the four vertexes of a rectangle shape. Such a configuration can form a close wave circulation if a source with frequency ω from $0.5437(2\pi c/a)$ to $0.5537(2\pi c/a)$ is excited in one of the two edges. Fig. 3 shows the calculated result for a wave frequency $\omega = 0.5517(2\pi c/a)$. The $\mathbf{E}_z$ field forms a clear rectangle loop in an anticlockwise direction. The loop leads to a resonance effect and concentrates the electromagnetic energy. Thus the whole path of the loop can be viewed as a ring resonator. Away from the resonator, all the fields decay to zero. We also notice that the field is exactly centrosymmetry. The close circulation in the ring resonator results from both the one-way property of the edge modes and the coupling effect of cavity. The circulation direction can be reversed just by changing the direction of applied magnetic fields. Compared with conventional ring resonator, this circulator has no port.

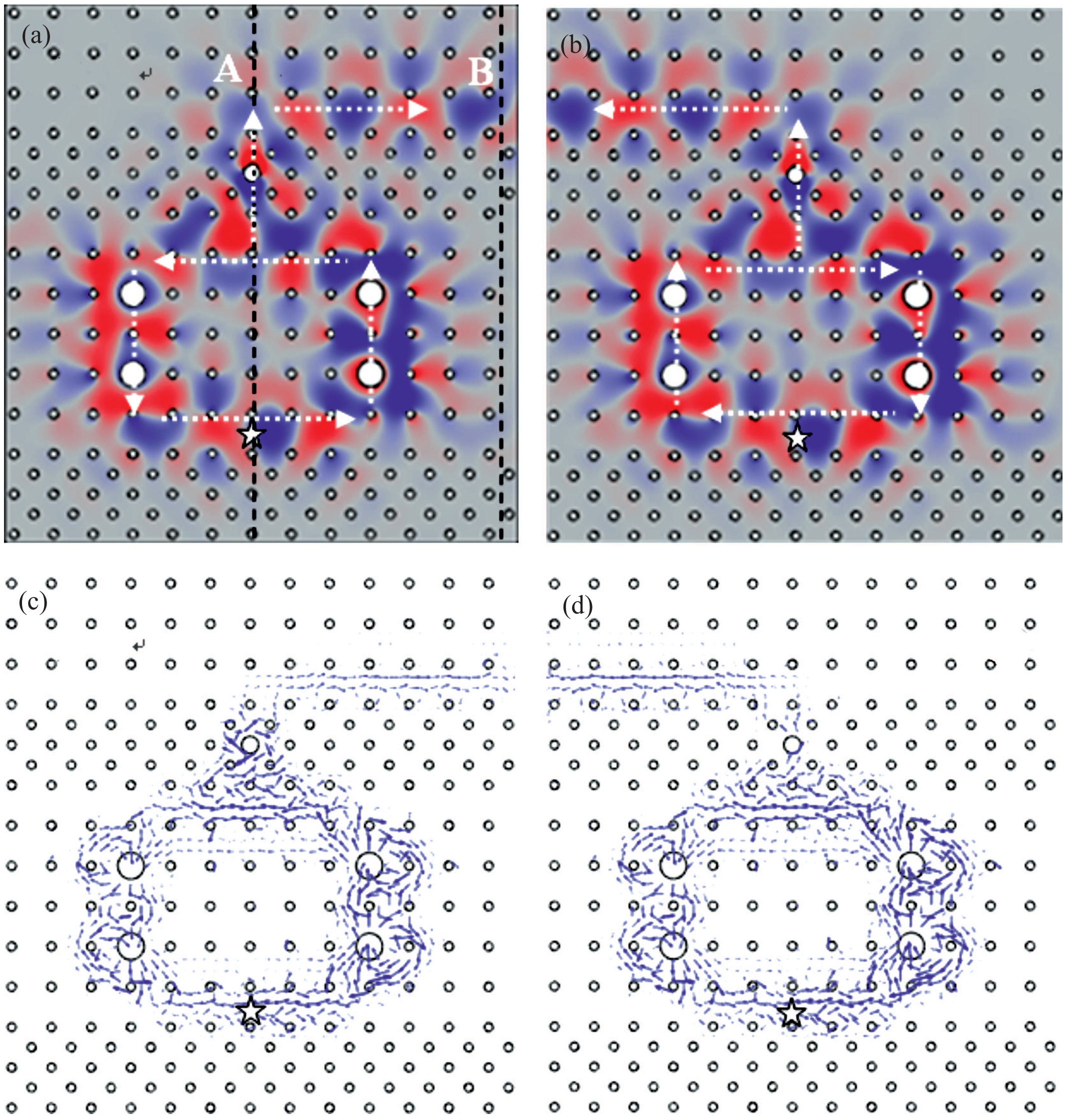

Fig. 4. (Color online) The excited $\mathbf{E}_z$ field from source at the lower edge of the loop. The loop is coupled to the upper edge channel through the cavity. The directions of applied magnetic fields on the two MO PC are the same (a) and opposite (b), respectively. The white arrows denote the propagation directions. (c), (d) – The distributions of the Poynting vectors correspond to a and b, respectively

The close ring resonator provides a potential to achieving an optical storage and writing system. When an electromagnetic signal is excited in the ring resonator, it will be saved. But the only ring resonator has no value because the signal can not be taken out. Thus we set up the third edge channel by adding another MO PC to the edge of the upper regular PC of Fig. 3. In the upper regular PC we set up a cavity by increasing a rod radius. Such a cavity is to couple the energy from the lower loop to the upper edge channel. To achieve a complete coupling at source frequency $\omega = 0.5517(2\pi c/a)$, we fine tune the defect rod radius to $0.212a$. The directions of applied magnetic fields to the two MO PCs are initially the same. When we place the source at the lower edge of the loop, the excited $\mathbf{E}_z$ field is shown in Fig. 4a. We see a clear wave tunnelling from the lower loop into the upper edge channel. The direction of wave in the upper edge channel is only to the right. Fig. 4c shows the energy flow by showing the distribution of the Poynting vectors. In the loop, although the intense scattering occurs around the four cavities, the average energy flow shows the anticlockwise circulation. In the upper edge channel the average directions of the Poynting vectors all point to the left showing clear one-way property. The direction of the upper edge channel can be reversed to the left just by changing the direction of applied magnetic fields on the upper MO PC. The result is shown in Fig. 4b and the corresponding energy flow is shown in Fig. 4d. Thus, the designed new compound structure has realized the reading functionality of storage system. Besides possessing the proeprty of nonreciprocity of conventional ring resonator, the current ring resonator has the property of the one-way edge modes of MO PCs, i.e., it is robust against the structure disorder along the edge channels.

In order to study the coupling efficiency of the ring resonator and the edge waveguide channel, we calculate the average electric energy density $\rho_E = 1/2\varepsilon(\mathbf{r})\varepsilon_0\overline{E(\mathbf{r})^2}$ along two lines denoted as A and B in Fig. 4a. Line A is just cross the source and the cavity in the regular PC, and line B is at the export port of the edge waveguide channel. The result is shown in Fig. 5 in which all the

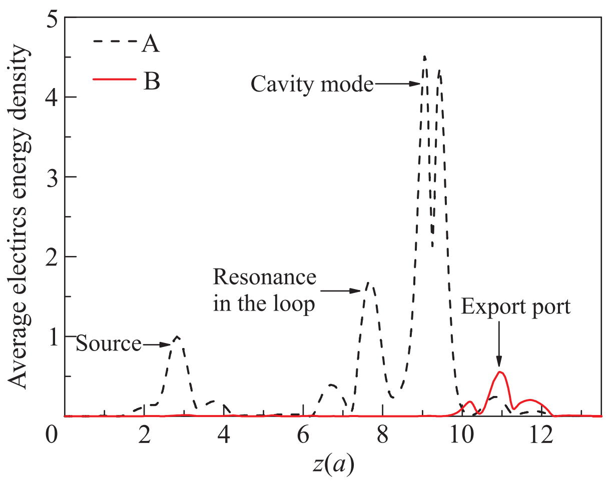

Fig. 5. (Color online) The average electric energy density along two lines denoted as A and B in Fig. 4a. All the values are in unit of the maximum value at the source. Line A is across the source and line B is $10.5a$ away from line A

values are in unit of the maximum value at the source. There are clear three main peaks corresponding to the source, the resonance in the ring loop and the resonance in the cavity on line A. The resonance peak in the ring loop shows that the wave energy is confined in the loop. The resonance peak in the cavity denotes that the cavity can accumulate enough energy to form a coupling between the loop and the waveguide. The resonance peak in the export port means that the wave energy is effectively coupled to the export waveguide through the cavity. The cavity mode has two sub-peaks representing a dipole state. The large energy density in the cavity means that an intense resonance occurs in the cavity. It is the resonance that transfers the energy into the upper waveguide channel from the ring. The coupling efficiency is found to be 0.6 obtained from the peak value at the export port.

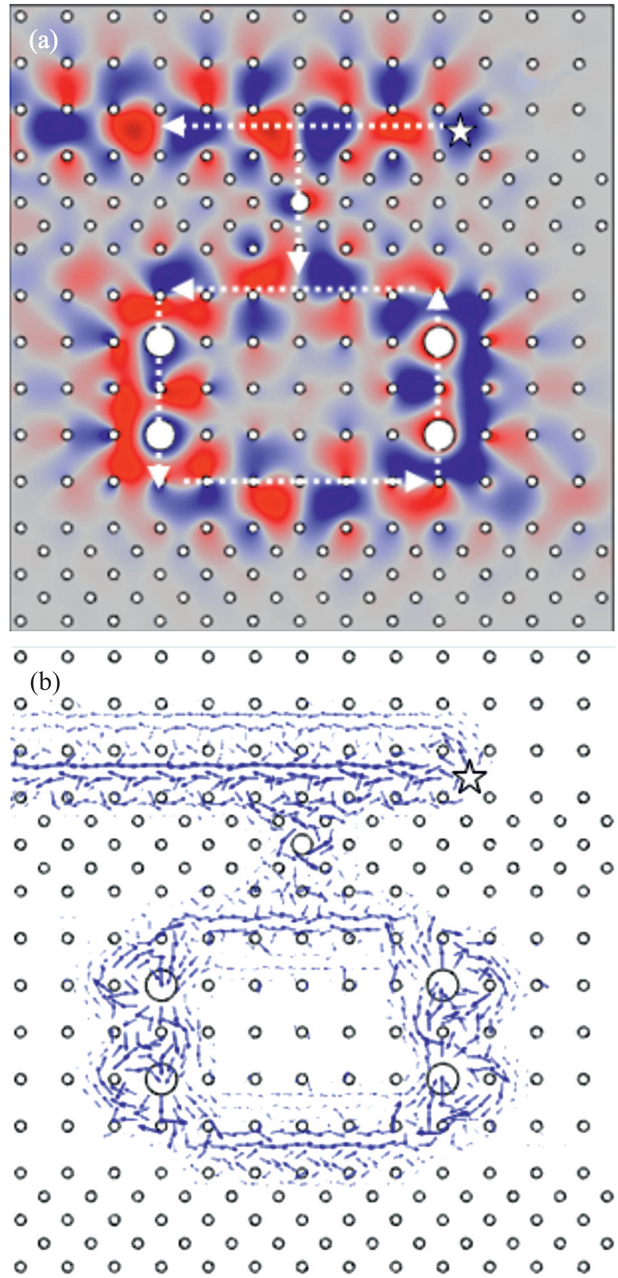

Fig. 6. (Color online) The excited $\mathbf{E}_z$ field from source at the upper edge waveguide (a) and the corresponding distributions of the Poynting vectors (b). All the white arrows denote the propagation directions

A complete storage system must have the functionality of writing which is also achieved through our disigned system. Basing on the structure of Fig. 4b, we set up a point source with frequency $\omega = 0.553(2\pi c/a)$ at the upper edge channel and make a numerical simulation. The results are shown in Fig. 6. The excited $\mathbf{E}_z$ field pattern in Fig. 6a forms a one-way flow to the left along the upper channel. But it is clear that some of the field has been dropped into the lower ring resonator through the coupling of cavity and the field in the resonator forms a circulation. The corresponding Poynting vectors are shown in Fig. 6b. It shows that the average energy flow in the ring shows the anticlockwise circulation. This process just denotes that a signal from a waveguide has been writted into the ring storage.

A similar study has been found in Ref. [9] in which a ring resonator is also coupled with a waveguide. The one-way circulation in the ring results from the unidirectional edge modes of MO PC. But the MO PC inside a regular PC has a small size, which degrades the effect of nonreciprocity and resonance. As a result, the coupling between the ring resonator and the waveguide is weaker than that in our designed system. As can be seen from Fig. 4 in Ref. [9], although the one-way transmission in the coupled waveguide is to the right, a weak wave occurs in the left direction. However, from Fig. 4 in this study, the one-way transmission in the coupled waveguide is complete to one direction.

IV. Conclusions. In this paper we construct a ring resonator system through the coupling of unidirectional edge modes and cavity modes. Given a proper structure parameters, the electromagnetic waves are traped in a close one-way circulation. Also, if the ring resonator is coupled with another one-way waveguide, the waves can be released or be written. The results may find their important applications in optical storage.

This work was supported by the Senior Talent Foundation of Jiangsu University under Grant # 13JDG003.

1. Y. A. Vlasov, M. O'Boyle, H. F. Hamann, and S. J. McNab, Nature **438**, 65 (2005).
2. Z. Wang, Y. D. Chong, J. D. Joannopoulos, and M. Soljacic, Nature **461**, 772 (2009).
3. Z. Wang and S. Fan, Opt. Lett. **30**, 1989 (2005).
4. V. R. Almeida, C. A. Barrios, R. R. Panepucci, M. Lipson, M. A. Foster, D. G. Ouzounov, and A. L. Gaeta, Opt. Lett. **29**, 2867 (2004).
5. S. Raghu and F. D. M. Haldane, Phys. Rev. A **78**, 033834 (2008).
6. F. D. M. Haldane and S. Raghu, Phys. Rev. Lett. **100**, 013904 (2008).
7. Z. Wang, Y. D. Chong, J. D. Joannopoulos, and M. Soljacic, Phys. Rev. Lett. **100**, 013905 (2008).
8. Z. Wang, Y. D. Chong, J. D. Joannopoulos, and M. Soljacic, Nature **461**, 772 (2009).
9. Z. Y. Wang, L. F. Shen, X. M. Zhang et al., J. Appl. Phys. **110**, 043106 (2011).
10. K. M. Ho and C. T. Chan, Phys. Rev. Lett. **65**, 3152 (1990).
11. K. M. Leung and Y. F. Liu, Phys. Rev. B **41**, 10188 (1990).